An Exploration of Discontinuous Time Synchronous Averaging for Helicopter HUMS Using Cruise and Terminal Area Vibration Data

Edward M. Huff and Marianne Mosher
NASA Ames Research Center

Eric Barszcz
QSS Group, Inc.
NASA Ames Research Center

Recent research using NASA Ames AH-1 and OH-58C helicopters, and NASA Glenn test rigs, has shown that in-flight vibration data are typically non-stationary [1-4]. The nature and extent of this non-stationarity is most likely produced by several factors operating simultaneously. The aerodynamic flight environment and pilot commands provide continuously changing inputs, with a complex dynamic response that includes automatic feedback control from the engine regulator. It would appear that the combined effects operate primarily through an induced torque profile, which causes concomitant stress modulation at the individual internal gear meshes in the transmission. This notion is supported by several analyses, which show that upwards of 93% of the vibration signal's variance can be explained by knowledge of torque alone. That this relationship is stronger in an AH-1 than an OH-58, where measured non-stationarity is greater, suggests that the overall mass of the vehicle is an important consideration. In the lighter aircraft, the unsteady aerodynamic influences transmit relatively greater unsteady dynamic forces on the mechanical components, quite possibly contributing to its greater non-stationarity.

In a recent paper using OH-58C pinion data [5], the authors have shown that in computing a time synchronous average (TSA) for various single-value metric computations, an effective trade-off can be obtained between sample size and measured stationarity by using data from only a single mesh cycle. A mesh cycle, which is defined as the number of rotations required for the gear teeth to return to their original mating position, has the property of representing all of the discrete phase angles of the opposing gears exactly once in the average. Measured stationarity is probably maximized because a single mesh cycle of the pinion gear occurs over a very short span of time, during which time-dependent non-stationary effects are kept to a minimum. Clearly, the advantage of local stationarity diminishes as the temporal duration of the cycle increases. This is most evident for a planetary mesh cycle, which can take several minutes to complete.

In the present study, a new approach is explored to minimizing the potentially detrimental effects of non-stationarity in signal averaging, by using data selectively from revolutions that satisfy *a priori* boundary constraints, e.g., on torque, speed, and so forth. The technique is called *discontinuous* time synchronous averaging (DTSA), because the revolutions entering into the average may be widely separated in time. By contrast, then, the conventional method may be thought of as *continuous* time synchronous averaging,

i.e., CTSA. It is evident that DTSA forfeits the advantage of assuring the presence of all phase angles in the mesh cycle in order to gain control over undesirable gear stress modulation.

Data for the present study were collected from Ames' helicopters in late 2001. As in previous studies mentioned above, data were collected using the NASA Ames *Healthwatch* system, which had been improved to keep continuous track of the shaft revolution count from the start of each data flight. Since the gears in the transmission are locked together, this assures that data from various recording epochs can be aligned analytically for averaging purposes.

As of this submission, extensive flight data that were recorded under both cruise and terminal area conditions are in the process of being indexed on a revolution-by-revolution basis of the main rotor. Once this is completed during the next few weeks, various averaging protocols will be compared statistically, which will allow evaluation of: (1) torque level and window size effects, (2) speed level and window size effects, (3) phase angles captured in the computed DTSAs, and (4) comparisons with conventional CTSA. The degree of uniformity obtained between sample averages computed with differing window constraints will be examined, as well as apparent effects on HUMS detection measures that are computed. Major contrasts will be discussed between cruise and terminal area results, as well as between averages computed on different flights.

REFERENCES

1. Huff, E.M., *et al. Experimental Analysis of Steady-State Maneuvering Effects on Transmission Vibration Patterns Recorded in an AH-1 Cobra Helicopter.* in *American Helicopter Society 56th Annual Forum.* 2000. Virginia Beach: American Helicopter Society.

2. Huff, E.M., *et al. Experimental Analysis of Mast Lifting and Bending Forces on Vibration Patterns Before and After Pinion Reinstallation in an OH-58 Transmission Test Rig.* in *American Helicopter Society 56th Annual Forum.* 2000. Virginia Beach: American Helicopter Society.

3. Huff, E.M., I.Y. Tumer, and M. Mosher. *An Experimental Analysis of Transmission Vibration Responses from OH-58c and AH-1 Helicopters.* in *American Helicopter Society 57th Annual Forum.* 2001. Washington D.C.

4. Huff, E.M., *et al., An Analysis of Maneuvering Effects on Transmission Vibrations in an AH-1 Cobra Helicopter.* Journal of the American Helicopter Society, 2002(January): p. 42-49.

5. Mosher, M., A.H. Pryor, and E.M. Huff. *Evaluation of Standard Gear Metrics in Helicopter Flight Operations.* in *56th Mechanical Failure Prevention Technology Conference.* 2002. Virginia Beach, VA.

An Exploration of Discontinuous Time Synchronous Averaging Using Helicopter Vibration Data

Edward M. Huff and Marianne Mosher
Computational Sciences Division
NASA Ames Research Center

Eric Barszcz
QSS Group, Inc.
NASA Ames Research Center

ABSTRACT

This paper explores discontinuous time synchronous averaging (DTSA) as a means for minimizing torque and related nonstationary effects on the frequency content of transmission vibration signals. Unlike conventional time synchronous averaging (TSA), DTSA averages only data for revolutions that occur in regions of a predefined state space. Using this approach, flight vibration data from the Ames AH-1S Cobra and OH-58C Kiowa helicopters were averaged for each state variable category combination of torque, residual shaft speed, and torque derivative. Category ranges were established empirically using quantile methods to assure an equal number of revolutions in each marginal distribution. The relative power associated with fundamental subsets of mesh frequencies in the power spectrum were found to change in a non-proportional but highly systematic manner within the state space. These results lend support to the use of DTSA methods in health monitoring systems, and point to the need for modeling the complex mesh frequency response relationships on a dynamic basis.

INTRODUCTION

Recent research using NASA Ames AH-1S Cobra and OH-58C Kiowa helicopters, and NASA Glenn test rigs [1-3], has shown that in-flight transmission vibration data are typically nonstationary. The nature and extent of this nonstationarity is most likely produced by several factors operating simultaneously. The aerodynamic flight environment and pilot commands provide continuously changing inputs, with a complex dynamic response that includes automatic feedback control from the engine regulator. It would appear that the combined effects operate primarily through an induced torque profile, which causes concomitant stress modulation at the individual internal gear meshes in the transmission. This notion is supported by several analyses, which show that 90% or more of the vibration signal's variance can be accounted for by torque alone. This relationship is appreciably stronger in an AH-1S than an OH-58C, where measured nonstationarity is also greater [4]. It has been suggested, therefore, that the mass of the vehicle is an important consideration. In the lighter aircraft, the unsteady aerodynamic influences transmit relatively greater unsteady dynamic forces on the mechanical components, quite possibly contributing to its greater non-stationarity.

In a recent paper using OH-58C pinion data [5], it was shown that in computing a time synchronous average (TSA) an effective trade-off can be obtained between the number of records used in the average and measured stationarity, by averaging data from a single "mesh cycle." A mesh cycle is defined as the number of rotations required for opposing gear teeth to return to their original mating positions. In the case of the pinion gear, this has the attractive property of representing all of the discrete phase angles of the opposing gear exactly once in the average. In this instance, measured stationarity is maximized because a single pinion mesh cycle occurs in less than a second, during which time-dependent effects are held to a minimum.

Presented at the American Helicopter Society 59th Annual Forum, May 7, 2003, Phoenix, Arizona.

As the length of the mesh cycle increases, however, the potential advantage of short duration stationarity quickly diminishes. At the opposite end of the transmission, for example, the planet gears take several seconds to realign within the fixed annulus. The situation becomes worse for the complete planetary mesh cycle, which takes several minutes to realign the planets with both the sun and ring gears. In the extreme, the transmission as a whole takes many hours to complete a full meshing cycle, which derives from the gear tooth counts being established as relatively prime numbers to minimize tooth pair interactions. Accordingly, in the case of the AH-1S Cobra, upwards of 150 flight hours would be required to return the transmission to an initial starting gear configuration—which rivals the transmission's maintenance cycle. Clearly, therefore, only for the shortest meshing cycles is it feasible to consider counterbalancing gear phase angles. For longer cycles, such an objective must be relaxed or overlooked. Moreover, because of the extended time involved, the focus of attention must turn to mitigating nonstationary effects.

In the present study, exploratory statistical analyses are presented to corroborate a novel method for minimizing the confounding effects of nonstationarity in signal averaging. In general, the approach involves averaging data selectively from revolutions that meet pre-determined state variable constraints, e.g., on torque, shaft-speed, aircraft attitudes, etc. It is referred to as *discontinuous time synchronous averaging* (DTSA), because the synchronous revolutions entering into an average are not necessarily contiguous and may come from different recording epochs, or even in theory different flights. The procedure contrasts strongly with the conventional method that may be thought of as *continuous* time synchronous averaging. It gives up the assurance that all phase angles will be represented in a given signal average in order to gain positive control over otherwise random gear stress modulations that normally occur in flight.

The basic principle underlying DTSA is at least conceptually related to the widespread notion that signal averaging is best done during certain maneuvering conditions, e.g., forward flight, climb, hover, etc. Most would agree that it is not the flight regime that is important, *per se*, but rather the near-ideal recording state it is hoped to produce [6].

OBJECTIVES

To explore the potential value of the DTSA concept for in-flight health monitoring, a new flight module called Healthwatch-2 is under development. It will be flown on the Army/NASA OH-58C during mid-2003 using software that will capture data for averaging that selectively falls within various parameter windows. The studies reported here are intended to explore which parameter combinations to use initially for such signal averaging, as well as methods to define category ranges.

Another objective of the present research is to use extensive flight data obtained from the Army/NASA AH-1S and OH-58C helicopters in late-2001 to study the within-signal effects that might be expected to take place in normal flight, and to answer certain fundamental questions about state variable effects on the overall power spectral distribution. In particular, there is strong interest in the detailed changes that take place in the *relative power* of the various mesh frequencies, and their harmonics, because this will provide greater insight into maneuvering effects that were previously reported only in terms of signal RMS [1-2].

The current analyses reflect a refinement of data preparation and signal analysis techniques, several of which were introduced in earlier papers. A continuing objective has been to subject *raw* triaxial data, rather than averaged RMS values, to three-dimensional rotation using principle-components analysis (PCA). This has the potential of: (1) consolidating the total variance onto uncorrelated axes more suitable for independent statistical analysis, and (2) simulating analytically a unique, and perhaps "optimal," physical accelerometer placement subsequent to operational sensor inspection or replacement.[1] Since synchronous time-domain averaging is most often done prior to computing conventional damage metrics, this will be done routinely with Healthwatch-2.

Finally, a related objective of the study is to explore further the advantages of power spectral averaging, particularly with regard to mesh-source variance components. This capability will also be present in Healthwatch-2 for continued research.

METHOD

Instrumentation

The AH-1S Cobra and OH-58C Kiowa aircraft were instrumented in the same manner reported in earlier studies [2, 4]. Accelerometers were mounted at the same locations on the transmissions,

[1] Several failures occurred during the course of this research that required accelerometer realignments.

although the x- and y-axis orientation of the triaxial was interchanged on the OH-58C by rotating it clockwise 90 degrees. The Healthwatch chassis was moved between the aircraft as required. To review, the Healthwatch system records eight channels of analog signals: six channels are dedicated to vibration recording; one channel is used to sample engine torque (a linear transformation of engine oil pressure); and one channel is used to sample a once per revolution tachometer signal from the main rotor shaft (adapted from each aircraft's AVA maintenance kit).

On the Cobra, specially machined hexagonal mounting brackets for two triaxial accelerometers (designated A and B) are attached to exposed threading on the casing bolts of the transmission housing. The x- and y-axes are oriented, more or less accurately, tangent and radial to the transmission respectively;[2] the z-axis naturally points downward in parallel with the rotor shaft. The accelerometers are physically closest to the lower planetary stage of the transmission.

On the OH-58C, matching mounting brackets for three uniaxial accelerometers and one triaxial accelerometer are attached with existing flange bolts surrounding the planetary annulus. Unlike the Cobra there is enough bolt length to allow the retaining nuts to be re-torqued over the bracket extensions. The three uniaxials and the z-axis of the triaxial are naturally oriented radially with respect to the planetary annulus. Using a special jig, the x- and y-axes are oriented tangent to the annulus gear and parallel to the rotor shaft respectively.

Experiment Design

Unlike previously reported flight studies [2], in which 14 maneuvering states were maintained under carefully sequenced test conditions, the present flights were intended to be more representative of a typical helicopter mission and were executed with relatively loose constraints. During the latter part of 2001 the AH-1S Cobra was flown on nine missions involving seven out-and-back flights and two terminal area flights; the OH-58C Kiowa was flown on six flights involving four out-and-back missions and two terminal area missions. The same test pilot flew each flight on both aircraft, accompanied by one of several copilots to operate the data recording equipment and fill out the test card. Due to different rotor speeds the number of revolutions recorded differed between the two aircraft. For this reason the current analyses include the first three out-and-back missions for the AH-1S, and the first two for the OH-58C. The remainder of the flight data will be analyzed and reported at a future time.

Summaries of the pilot's test cards (Table 1) show that the legs of the flight plans involve different altitude-airspeed combinations and transitions between them. Broadly speaking, the flights contain both cruise and terminal-area data. The test cards were only used as general guidelines, however, and the pilots occasionally changed indicated altitude for the second half of the mission depending on local conditions. No attempt was made to prevent or inhibit maneuvering variations that became necessary from flight to flight, or make local changes due to varying wind or weather conditions. Except for the first OH-58C flight, pilot notes were not maintained of the particular recording epochs that occurred for successive legs of each mission. Since Healthwatch was programmed to automatically take 34 sec. recording as often as possible, it proved infeasible to monitor and log computer record numbers from the hand-held display. Additionally, the number of data records obtained from each flight varied considerably based on its duration and the method used to download and store data.

Data Reduction

Flight data were reduced in several stages that produced highly compressed summary files. These are archived and available for continued analyses. During the first stage several global statistics were computed from the raw data for all reference flights combined. Most importantly this yielded the raw covariance matrix of the x, y, and z channels of each triaxial accelerometer. The covariance matrix was then used to calculate an idealized rotation scheme using principal components analysis (PCA). The ensuing normalized eigenvalues indicate the proportion of total variance accounted for by each principal component (PC). The eigenvector matrix contains the linear weights needed to rotate the original axes to an "optimal" orientation (Table 2). It may be seen that for each aircraft the largest rotation weights lie along the main diagonal, which means that the optimal orientations of the accelerometers largely conformed to their physical mountings.

At the next stage, extensive data compression was done on a revolution-by-revolution basis of the main rotor shaft—which corresponds with the rotation of the uppermost planetary carrier. Using the tachometer channel to detect the beginning and ending points for each shaft revolution, the data for each channel were then interpolated to a common

[2] The x- and y-axis orientations were established manually without the aid of a mounting jig.

number of samples (2^{13} = 8192) using a cubic spline algorithm. The number of sampled data points within each revolution was used to determine its RPM value. A large number of sample statistics were then calculated for the torque, uniaxial, triaxial and PC score channels. The subset used in this study is summarized in Table 3.

Although it would be possible to use any combination of flight parameters to establish a state space, it was decided to limit the initial DTSA investigation to only variables associated with torque and shaft speed. Because no IEEE 1553 attitude data were available for the OH-58C, this allowed the two vehicles to be compared on an equivalent basis.

Table 1: Out-and-Back Mission Flight Conditions

OH-58C Out-and-Back Mission Flight Cards 2001, Flights {1-4}			AH-1S Out-and-Back Mission Flight Cards 2001, Flights {1-4, 6, 8-9}		
Pressure Altitude	Target KIAS	Flight Condition	Pressure Altitude	Target KIAS	Flight Condition
3500	100	Cruise Flight	NA	NA	Hover (4 min)
3500	75	Cruise Flight	1000	120	Transition NUQ-to-East Bay
3500	45	Cruise Flight	1000-3500	120	Climb to 3500 ft MSL
3500-9500	45	Climb to 9500 ft MSL	3500	120	Cruise Flight (7 min)
9500	45	Cruise Flight	3500	95	Cruise Flight (7 min)
9500	60	Cruise Flight	3500	60	Cruise Flight (7 min)
9500	75	Cruise Flight	3500-7500	80	Climb to 7500 ft MSL
9500-8500	75	Descend to 8500 ft MSL and Reverse course	7500	60	Cruise Flight (7 min)
8500	85	Cruise Flight	7500	75	Cruise Flight (7 min)
8500	65	Cruise Flight	7500	90	Cruise Flight (7 min)
8500	45	Cruise Flight	7500-6500	90	Descend to 6500 ft MSL and Reverse course
8500-2500	85	Descend to 2500 ft MSL, Collective full down	6500	90	Cruise Flight (7 min)
2500	85	Cruise Flight	6500	75	Cruise Flight (7 min)
2500	65	Cruise Flight	6500	60	Cruise Flight (7 min)
2500	45	Cruise Flight	6500-2500	60	Descend to 2500 ft MSL, Collective full down
2500-1000	100	Descend to 1000 ft MSL After Sunol Pass	2500	60	Cruise Flight (7 min)
1000	100	Transition Sunol-to-NUQ	2500	95	Cruise Flight (7 min)
NA	NA	Hover	2500	120	Cruise Flight (7 min)
			2500-1000	120	Descend to 1000 ft MSL After Sunol Pass
			1000	120	Transition Sunol-to-NUQ
			NA	NA	Hover

Underlying Statistical Concepts

Spectral Decomposition: Based on *Parseval's theorem,* in the time domain the Mean Square (MS) of a signal of length N is equal to its total power in the frequency domain [7]. Since total power represents the sum of the spectral energy over all frequencies, changes in variance must reflect the aggregate effects of relative changes in strength of the individual frequency

components. Signals having the same MS do not necessarily have the same underlying power spectrum, and conditions that change the MS by a given amount may in theory produce different spectral distributions. These effects require detailed analyses, which are aided by the following fundamental relationships:

$$MS = (RMS)^2 = \mu^2 + \sigma^2 = \sum_{i=0}^{N/2} P_i$$

$$\mu^2 = P_0 = 0$$

where μ and σ are the mean and standard deviation of the infinite time series, respectively, P_i is the power of the i^{th} frequency band, and $N/2$ is the number of bands. For an ideal vibration signal the mean is zero. Therefore, by substitution and induction:

$$MS = (RMS)^2 = \sigma^2 = \sum_{i=1}^{N/2} P_i = \sum_{i=1}^{N/2} \sigma_i^2$$

and for $0 < i \leq N/2$

$$P_i = \sigma_i^2$$

From a statistical perspective, therefore, Fourier analysis represents a linear decomposition of the total signal variance, σ^2, with the result that it isolates the variance associated with each individual frequency. For statistical analysis, a useful corollary is that the variance and degrees-of-freedom (df), associated with any arbitrary *set* of source frequencies can be expressed:

$$\sigma^2_{Source} = \sum_{i \in Source} P_i = \sum_{i \in Source} \sigma_i^2$$

$$df_{Source} = 2 \sum_{i \in Source} df_i$$

Because addition is commutative, frequency component variances may be grouped at will, e.g., mesh frequencies, harmonics, sidebands, etc. For statistical purposes, each frequency in the resulting sets is associated with two degrees-of-freedom due to the symmetry of the discrete Fourier transform.[3]

[3] The last band, $P_{N/2}$, has only one degree of freedom.

Table 2: Percent Variance per PC Axis and Rotation Weights

	PC Axis	Percent Variance	Rotation Weight Matrix x	y	z
AH-1S Triaxial A	1	64.694	-0.933	-0.177	0.314
	2	32.529	0.217	-0.971	0.097
	3	2.777	0.288	0.158	0.944
AH-1S Triaxial B	1	74.735	-0.936	0.011	0.351
	2	22.314	0.055	-0.983	0.177
	3	2.951	0.347	0.185	0.920
OH-58 Triaxial	1	70.96	-0.995	-0.055	0.083
	2	26.02	0.072	-0.973	0.221
	3	3.01	0.068	0.225	0.972

Table 3: Properties Calculated per Shaft Rotation (partial list)

Torque	Shaft Speed	Power Spectral Energy
Mean	RPM	Total
First Derivative	Residual RPM	Upper Planetary
		Lower Planetary
		Engine Mesh
		Pinion Mesh

Synchronous Power Spectral Averaging:[4] As discussed above, the objectives of the present study are focused on state variable effects on the signal's power spectral distribution, and, in particular, the relative changes that may take place as a result of unpredictable nonstationary influences during flight. Although most damage detection metrics, e.g., FM0, FM4, N6A, etc, are computed on time-domain averages, the present study's objectives were much better served by averaging in the frequency domain. This has the advantage of addressing spectral content issues directly.

The total vibration power in each signal was partitioned into separate gear components and a residual. For the AH-1S, the components are the upper planetary system, lower planetary system, pinion gear mesh and the residual. For the OH-58C, the components are the planetary

[4] "Synchronous" reflects that tachometer pulses are used to separate the time-series data.

gear system, pinion gear mesh, turbine output gear and residual. The power attributed to each component is the sum of the power in all frequency spectrum bins associated with that component.

State Variables and Quantile Categorization of Continuous Data: The results presented in this paper are based upon categorizing three state variables, i.e., torque (Q), residual-RPM (RRPM), and, torque derivative (Q') into eight ordinal categories. RRPM was selected as a state variable rather than RPM because of the strong negative correlation between Q and RPM (see Table 5), particularly for the OH-58C. RRPM values are computed as deviations from the linear regression line of RPM on Q.[5]

The categories for each state variable were established by computing the (seven) octile boundaries of the distributions combined over all flights. The rationale for using quantile methods, rather than simply dividing the overall range of the variables into eight equally spaced intervals, is that they are not distributed uniformly. Hence, using equal scale intervals would result in a markedly different number of shaft revolutions falling into each category on a marginal basis. Eight categories were selected as an initial compromise between scale resolution and empirical frequency counts. Since the DTSA methodology involves taking averages for *combinations* of parameter categories, enough incidents must occur naturally during flight to trigger an averaging operation. Future studies of a more refined nature may establish that a different number of categories are optimal for the state variables.

RESULTS

Distribution of Variables and Categorization: Histograms of Q, RRPM, and Q' are shown in Fig. 1 for the combined flights. Q is notably multimodal for each aircraft. Summary statistics for each distribution (Table 4) include the seven specific percentile points used to classify these variables for signal averaging. Although the number of revolutions in each marginal category is about equal, due to the use of quantile methods, the number falling into each two- and three-category *combination* varied widely. This circumstance resulted from the inter-correlation structure. For example, for negatively correlated variables, simultaneously high or simultaneously low combinations do not occur as frequently as low and high combinations. Since Q' and RRPM were forced to have a zero correlation, (Table 5), the cross-category counts were somewhat equalized by using RRPM as a state variable. The unequal counts were still quite prevalent, however, probably due to complex partial correlation structure with other hidden or unmeasured variables. Within cell frequencies also varied from flight to flight due to unpredictable flying conditions, which was especially true for the OH-58C. The two- and three-dimensional frequency tables are too extensive to include in this report, but are being examined to better understand the complex dependencies involved.

Table 4: Statistics and Percentile Values of Category Variables

AH-1S Cobra	Q	Q'	RRPM
N	34379	34379	34379
Mean	45.312	-0.002	-0.002
Median	41.240	0.000	0.000
St. Dev.	14.608	0.463	0.463
Range	87.060	11.310	11.310
Percentiles			
12.50	32.910	-0.230	-0.230
25.00	35.900	-0.090	-0.090
37.50	38.890	-0.040	-0.040
50.00	41.240	0.000	0.000
62.50	45.350	0.040	0.040
75.00	54.630	0.090	0.090
87.50	61.840	0.220	0.220

OH-58 Kiowa	Q	Q'	RRPM
N	29009	29009	29009
Mean	54.689	0.006	0.000
Median	52.370	0.000	-0.274
Std. Dev.	16.244	0.261	2.079
Range	85.190	8.070	33.487
Percentiles			
12.50	40.813	-0.180	-1.667
25.00	43.540	-0.090	-1.032
37.50	48.610	-0.040	-0.591
50.00	52.370	0.000	-0.274
62.50	59.490	0.040	0.083
75.00	66.660	0.080	0.644
87.50	75.370	0.170	1.376

[5] Quadratic and higher order regression did not improve predictive power.

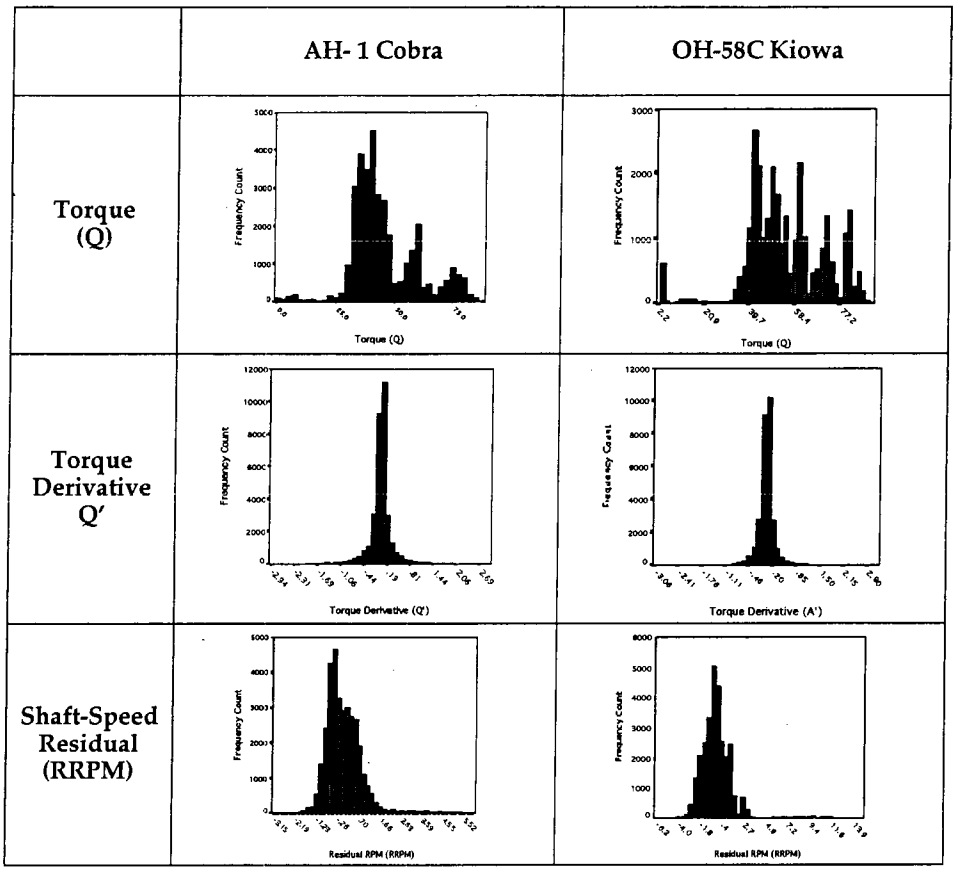

Figure 1: State variable distributions for combined flights.

Frequency Domain Signal Averaging: As discussed above, synchronous averaging in this study is focused upon grouped mesh frequencies in the power spectra for each of the specimen aircraft. Based on the use of eight categories for each of three parameters, as many as $(8)^3 = 512$ different averages might have been computed, provided that at least one revolution actually occurred for each combination. Had the three-state combinations been distributed uniformly there would have been about 67 each for the Cobra, and 57 each for the Kiowa (Table 5). Due to the complex state dependencies discussed above, however, the observed sample frequencies were not uniformly but exponentially distributed. Many combinations occurred infrequently, and a few combinations occurred relatively often.

For use in a real in-flight Health and Usage Monitoring System (HUMS), a set of parameter combinations would probably be selected, and a fixed sample size used for averaging. For the present exploratory investigation, however, a single average was computed for each category combination, with whatever samples appeared, so as to obtain global insight into the underlying functional relationships. Since the statistical precision varied a great deal based on sample size, therefore, detailed statistical inferences are not warranted. However, to assure that the overall findings are not artifacts, several partial correlation analyses were done correcting for sample size. Although not reported here, in no instance did sample size variations appear to change the basic relationships seen at a macro level.

Explanation of Signal Averaging Summary Charts: Presenting data simultaneously from a huge number of signal averages is daunting. Accordingly, visualization is aided by the use of

charts that organize averages from the category combinations in a *nested* fashion. It should be kept in mind that nesting order greatly influences the visual pattern produced, and is therefore specified in the figure captions where necessary. For example, clustering the Torque-Derivative (Q') within RPM-Residual (RRPM) within Torque (Q) means that reading from left to right on the chart, each of the eight torque categories has nested within it the eight RPM-residual categories, and within each of these is nested the eight torque-derivative categories—for an upper limit of 512 averages. Hence, in this example the nesting would be stated symbolically "Q > RRPM > Q'." By convention, each category variable is ordered from low index value to high. In the charts, vertical lines isolate the flights. Therefore, Fig. 2 compactly represents as many as 512 x 3 = 1536 averages for the Cobra and 512 x 2 = 1024 averages for the OH-58C.

Total Power or (MS): The panels in Fig. 2 show that for each aircraft total power generally tends to increase with increasing torque level. For the AH-1 individual PCs are well organized and total power follows a similar increasing relationship with torque. Within each torque-level category, total power is further modulated by the RRPM as well as Q', as can be seen by the saw-tooth pattern.

Based on separate analyses, not shown here due to space limitations, when averaging is done on two-category combinations the relationship between total power and RRPM is clearly monotonic decreasing, with power decreasing with RRPM at each fixed level of torque, and two-valued parabolic (i.e., an inverted "U") with respect to Q'. The negative relationship between MS and RRPM is somewhat confusing in view of the negligible first order correlation between these two variables. Apparently, this aspect only becomes evident when torque level is held constant, and, hence, a deeper understanding will require a more thorough partial correlation analysis. There is a strong hint, due to the parabolic relationship between MS and the Q', that the absolute value of Q' may prove to be a better state variable to use. (Since substituting this in the present study would primarily reduce the number of Q' categories from eight to four, the data were not reanalyzed on this account.)

For the OH-58C, PC-1 is notably different from this overall trend, and has essentially a flat response with torque level that is modulated in some joint manner by Q, RRPM and Q'. From the rotation matrix (Table 2) it is evident that PC-1 is minimally changed from the raw x-axis (unlike PC-2 and PC-3, which trade-off variance between the raw y- and z-axes.) On the OH-58C the x-axis (or PC-1) is oriented tangent to the planetary annulus, where it was reported in an earlier study [4] that a very large torsional vibration was discovered.[7] The reason for this remains unclear, but there is little doubt that this excitation is what is consolidated onto PC-1, and largely separated from PC-2 and PC-3.

To better appreciate the relative contribution of the state variables to the total mesh energy of the transmission, the sum-of-squares around the grand mean of the experiment was partitioned by a hierarchical fixed-effects analysis of variance (ANOVA) for each uniaxial or PC-axis [8].[8] For the Cobra, (Table 6) it is clear that a very large proportion of variability (75-86%) is accounted for by the Q state alone. Subtracting this effect, the remaining statistical model accounts for <10% of the variability in total power. The unaccounted variability is designate the residual.

Table 5: Category Variable Correlations

AH-1S Cobra				
N = 34379	Q	Q'	RRPM	RPM
Torque (Q)	1	-.006	0	**-.543**
Torque Derivative (Q')	-.006	1	-.408	-.339
Residual Speed (RRPM)	0	-.408	1	.840
Shaft Speed (RPM)	-.543	-.339	.840	1
OH-58C Kiowa				
N = 29009	Q	Q'	RRPM	RPM
Torque (Q)	1	-.027	0	**-.837**
Torque Derivative (Q')	-.027	1	-.234	-.106
Residual Speed (RRPM)	0	-.234	1	.547
Shaft Speed (RPM)	-.837	-.106	.547	1

[7] Torsional vibration was inferred after the sensor was relocated to several sites and strong tangential responses persisted.

[8] The method is used descriptively. Results are affected by the order of source extraction, and interaction terms are pooled within the residual if null frequencies occur.

For the OH-58C (Table 7) the situation is largely different in that uniaxial channels differ considerably from one another, and Q accounts for less variability on all channels (22-75%). For the first uniaxial, Q accounts for very little variation (22%), but in this instance the other variables and interaction terms account for 16%. Consistent with the earlier discussion, PC-1 has notably little variation accounted for by Q (30%), and PC-2 and PC–3 have higher Q contributions; PC-2 bears some similarity to the AH-1S type of response pattern shown in Fig 5. It should be emphasized from Tables 6 and 7 that much less residual variation is evident for the Cobra (10–22%), and much more is evident for the Kiowa (33–65%). Vibration on the OH-58C is much less predictable overall.

Relative Mesh Power: A primary motivation for conducting the present study was to investigate the relative changes in power that take place among the internal mesh frequencies under different state variable conditions. In order to perform this analysis, absolute mesh power was re-expressed as a proportion of the total, or *relative power*, including a residual to sum to 1.0.

Partitioning of the mesh frequency components of the two helicopters corresponded with the analysis reported by Huff, Tumer, et. al. [4]. The AH-1 Cobra power spectra are partitioned by the upper and lower planetary systems, and the pinion. As mentioned above, the OH-58C spectra are partitioned by the planetary, pinion, and engine frequencies. The remaining power for all unidentified frequencies is clustered into a residual term.

Fig. 3 demonstrates how the relative power distributions change with state variables. Due to space limitations, only the three PC axes for accelerometer "A" on the AH-1S, and the three PC axes on the OH-58C are shown for comparison.

Overall, the relative proportion of total power attributable to the mesh frequencies combined increases with absolute power. This is evidenced by the downward trend in the residual relative power on the charts. The picture is considerably more complicated, however, with regard to the individual mesh frequencies. In all cases, there is a tradeoff in relative energy between the meshes, although the pattern differs between the two aircraft.

On the AH-1, for each PC the upper planetary and pinion jointly trade power with the *lower* planetary, which contains the lion's share of relative energy throughout. For the most part, the upper planetary and pinion remain proportional, although more relative power is present for the upper planetary, and the pinion is much more strongly modulated by RRPM and Q′ effects.

On the OH-58 the planetary is consistently the dominant reservoir for relative power, and the pinion and engine meshes trade second place positions from PC-2 to PC-3. On each PC an obvious tradeoff occurs between planetary power and pinion or engine power. Again, clear modulating effects can be seen for the RRPM and Q′ classification variables.

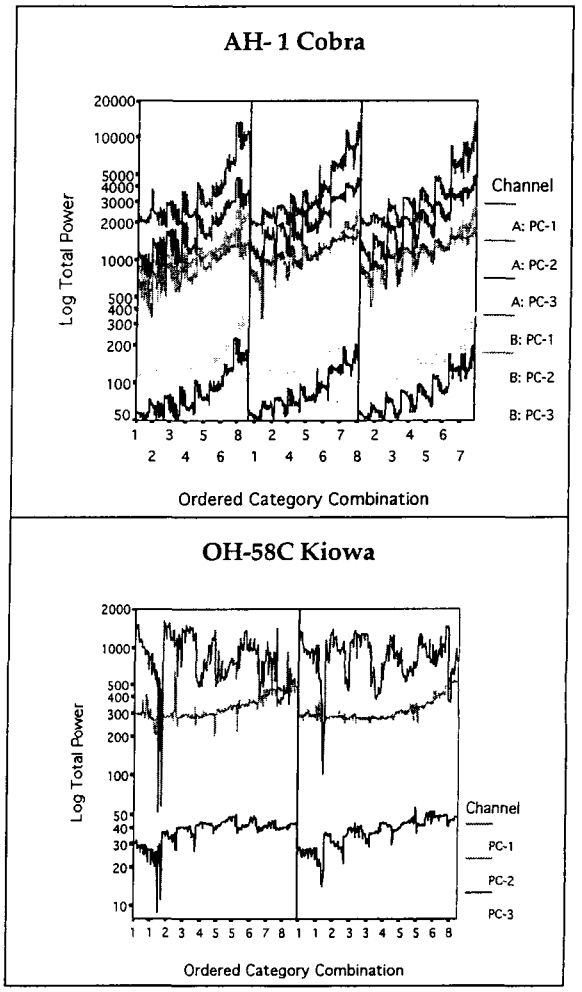

Figure 2: Average total power for each Principal Component in category order Q > RRPM > Q′.

The effects of very strong OH-58C torsional vibrations noted above on PC-1 are now revealed to be composed of large power swings in planetary relative power, accompanied primarily by trades with engine power. Pinion power modulates with engine power, which is not too surprising since the engine's energy is transferred to the transmission system via the pinion shaft.

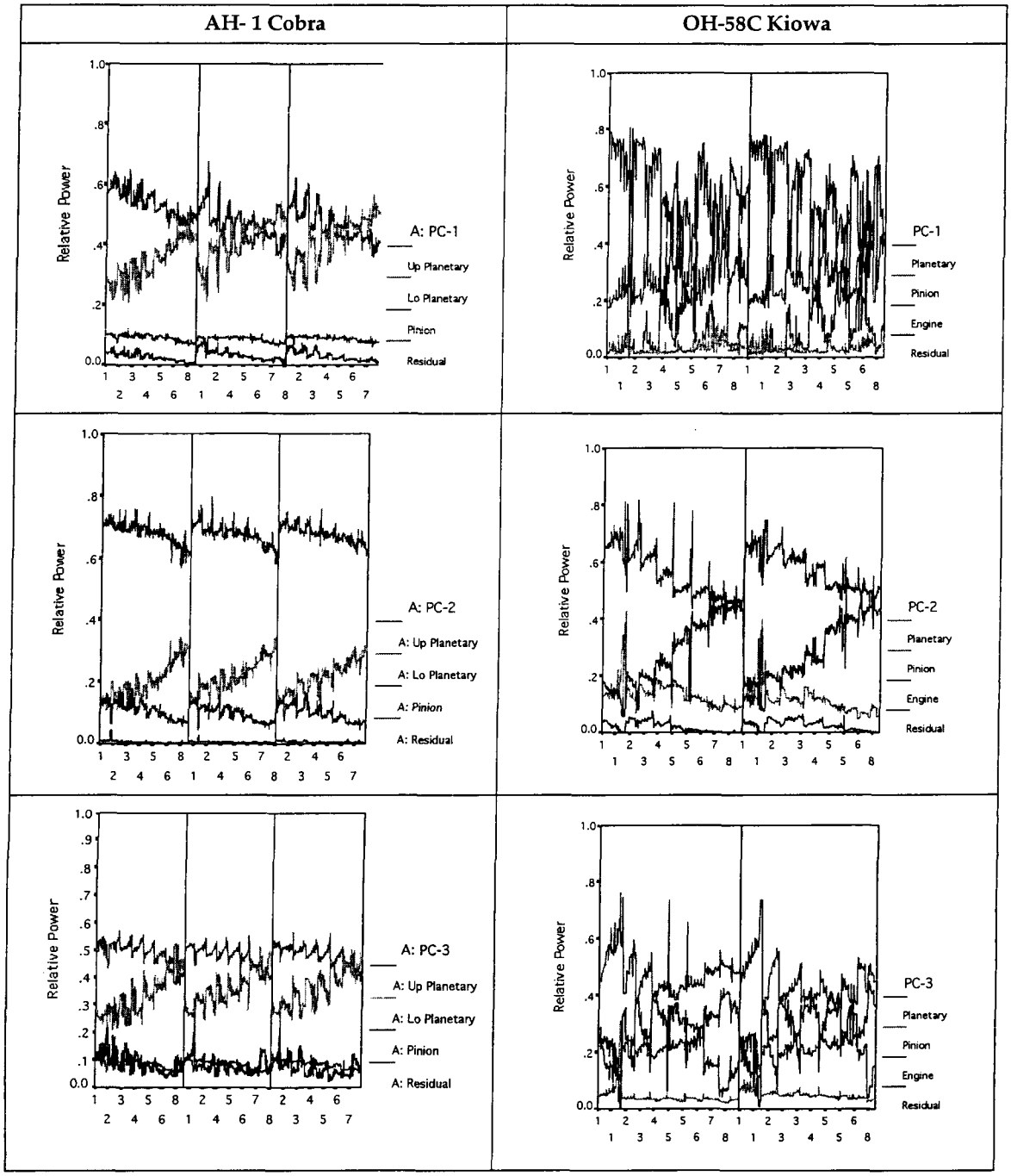

Figure 3: Relative Mesh Power by Principal Components in nested category order Q > RRMS > Q'.

Table 6: Proportion of Variability for AH-1 Cobra Spectral Power

AH-1 Cobra	Triaxial A PC1	Triaxial A PC-2	Triaxial A PC-3	Triaxial B PC-1	Triaxial B PC-2	Triaxial B PC-3
1-Way Total	0.774	0.723	0.854	0.864	0.822	0.862
Torque (Q)	0.750	0.691	0.830	0.849	0.805	0.852
Residual RPM (RRPM)	0.016	0.017	0.015	0.006	0.007	0.004
Derivative of Torque (Q')	0.009	0.014	0.009	0.009	0.011	0.006
2-Way Total	0.032	0.045	0.030	0.028	0.035	0.027
Q x RRPM	0.010	0.024	0.011	0.009	0.023	0.015
Q x Q'	0.012	0.012	0.009	0.011	0.008	0.007
RRPM x Q'	0.005	0.005	0.004	0.004	0.004	0.003
3-Way Total	0.014	0.015	0.008	0.008	0.008	0.006
Total Model	0.070	0.092	0.063	0.051	0.060	0.043
Minus Q Effect	0.180	0.217	0.107	0.100	0.135	0.106
Residual						

Table 7: Proportion of Variability for OH-58C Kiowa Spectral Power

OH-58C Kiowa	Uniaxial 1	Uniaxial 2	Uniaxial 3	Triaxial PC-1	Triaxial PC-2	Triaxial PC-3
1-Way Total	0.381	0.557	0.519	0.344	0.766	0.663
Torque (Q)	0.218	0.535	0.464	0.298	0.751	0.622
Residual RPM (RRPM)	0.151	0.005	0.049	0.038	0.012	0.032
Derivative of Torque (Q')	0.013	0.016	0.006	0.008	0.003	0.009
Total Model	0.163	0.022	0.055	0.046	0.015	0.041
Minus Q Effect	0.619	0.443	0.481	0.656	0.234	0.337
Residual						

CONCLUSIONS AND FUTURE RESEARCH

In the present study an initial effort has been made to explore the viability of discontinuous time-synchronous averaging (DTSA). This is envisioned, on the one hand, as a method to mitigate the nonstationary effects that are produced during dynamic flight, and, on the other hand, as a means to reveal the nature of power spectral density changes that occur in flight. The underlying notion is that the torque profile induced by flight maneuvering, combined with automatic engine speed regulation, dynamically modulates gear stresses that are reflected in a predictable pattern of changes to the vibration spectrum.

The results clearly provide evidence that highly systematic changes take place within the power spectrum as the aircraft moves though the state space defined by torque, torque derivative, and residual shaft speed. In addition, it is evident that the vibration picture within the transmission involves continuous tradeoffs in relative power between mesh frequencies. Although a unifying model that would account these results is not immediately at hand, it is hoped that in the near future this will be addressed from a physics or control theoretic perspective, which might incorporate unifying conservation principles.

From a practical HUMS point of view, the present findings suggest that regions of the state space may identify spectral responses that are essentially independent of the specific maneuvers that produced them. If confirmed, this would obviate the need for traditional "regime recognition" schemes that are both difficult to implement and questionable with regard to producing the ideal conditions that are

desired for signal averaging and related analyses. Future analytical research with AH-1S legacy data will be used to validate this.

Although it did not prove possible to include a comprehensive analysis in the present study, it is conceivable that the reported negative exponential distribution of sample sizes for the 512 states reflects a useful propensity for the aircraft to operate in certain regions of the multi-dimensional state space and not in others. Accordingly, the current data will be used to determine if "typical" state space regions of the aircraft provide a natural basis for selective averaging. In all these respects, then, the present study essentially reflects work in progress to determine the promise of DTSA.

Acknowledgements

The authors would like to express gratitude to Mr. Larry Cochrane, Sigpro, for highly professional aircraft instrumentation and data collection support. Thanks is also extended to Mr. Munro Dearing, III, who piloted both aircraft through daunting hours of flight tests, and in general to the staff of the Army/NASA Flight Projects Office headed by Major David Arterburn. Finally, we would like to belatedly recognize the encouragement and support provided over many years by Mr. Martin Maisel, who we greatly miss in retirement.

REFERENCES

1. Huff, E.M., *et al. Experimental Analysis of Steady-State Maneuvering Effects on Transmission Vibration Patterns Recorded in an AH-1 Cobra Helicopter.* in *American Helicopter Society 56th Annual Forum.* 2000. Virginia Beach: American Helicopter Society.
2. Huff, E.M., *et al., An Analysis of Maneuvering Effects on Transmission Vibrations in an AH-1 Cobra Helicopter.* Journal of the American Helicopter Society, 2002(January): p. 42-49.
3. Huff, E.M., *et al. Experimental Analysis of Mast Lifting and Bending Forces on Vibration Patterns Before and After Pinion Reinstallation in an OH-58 Transmission Test Rig.* in *American Helicopter Society 56th Annual Forum.* 2000. Virginia Beach: American Helicopter Society.
4. Huff, E.M., I.Y. Tumer, and M. Mosher. *An Experimental Analysis of Transmission Vibration Responses from OH-58c and AH-1 Helicopters.* in *American Helicopter Society 57th Annual Forum.* 2001. Washington D.C.
5. Mosher, M., A.H. Pryor, and E.M. Huff. *Evaluation of Standard Gear Metrics in Helicopter Flight Operations.* in *56th Mechanical Failure Prevention Technology Conference.* 2002. Virginia Beach, VA.
6. Teal, R.S., *et al. Regime Recognition for MH-47E Structural Usage Monitoring.* in *American Helicopter Society 53rd Annual Forum.* 1997. Virginia Beach, VA: American Helicopter Society.
7. Oppenheim, A.V., A.S. Willsky, and I. Young, *Signals and Systems.* 1983, Englewood Cliffs, NJ: Prentice-Hall.
8. Scheffé, H., *The Analysis of Variance.* First ed. 1959, New York: Wiley. 477.